

# Human Taste Cells Express ACE2: a Portal for SARS-CoV-2 Infection

Running Title: Persistence of SARS-CoV-2 in Human Taste Buds

Máire E Doyle, Ph.D.<sup>1</sup>, Ashley Appleton, B.Sc.<sup>1</sup>, Qing-Rong Liu, Ph.D.<sup>1</sup>, Qin Yao, M.D.<sup>1</sup>, Caio Henrique  
Mazucanti, Ph.D.<sup>1</sup>, Josephine M Egan, M.D.<sup>1</sup>

Address Correspondence to:

Josephine M Egan, M.D.

<sup>1</sup>National Institute on Aging/Intramural Program,

251 Bayview Blvd,

Baltimore MD 21224

[eganj@grc.nia.nih.gov](mailto:eganj@grc.nia.nih.gov)

and

Máire E Doyle, Ph.D.<sup>1</sup>

[doyleme@nih.gov](mailto:doyleme@nih.gov)

# of Text Pages 9 (excluding references and legends)

# of Tables 2

# of Figures 2

Funded by the NIA/NIH intramural research program. Project Number 1ZIAAG000291-13, JME.

The authors declare that there are no conflicts of interest.

## 25 Abstract

26 Loss and changes in taste and smell are well-reported symptoms of SARS-CoV-2 infection. The virus targets  
27 cells for entry by high affinity binding of its spike protein to cell-surface angiotensin-converting enzyme- 2  
28 (ACE2). It was not known whether ACE2 is expressed on taste receptor cells (TRCs) nor if TRCs are infected  
29 directly. Using an *in-situ* hybridization (ISH) probe and an antibody specific to ACE2, it seems evident that  
30 ACE2 is present on a subpopulation of specialized TRCs, namely, PLC $\beta$ <sub>2</sub> positive, Type II cells in taste buds in  
31 taste papillae. Fungiform papillae (FP) of a SARS-CoV-2+ patient exhibiting symptoms of COVID-19,  
32 including taste changes, were biopsied. Based on ISH, replicating SARS-CoV-2 was present in Type II cells of  
33 this patient. Therefore, taste Type II cells provide a portal for viral entry that predicts vulnerabilities to SARS-  
34 CoV-2 in the oral cavity. The continuity and cell turnover of the FP taste stem cell layer of the patient were  
35 disrupted during infection and had not fully recovered 6 weeks post symptom onset. Another patient suffering  
36 post-COVID-19 taste disturbances also had disrupted stem cells. These results indicate that a COVID-19 patient  
37 who experienced taste changes had replicating virus in their taste buds and that SARS-CoV-2 infection results  
38 in deficient stem cell turnover needed for differentiation into TRCs.

## 17 **Introduction**

18 As many as 80% of people infected with SARS-CoV-2 report taste and smell changes, as well as changes in  
19 overall oral sensitivity to commonly used condiments and spices. The constellation of sensory symptoms can  
20 precede systemic symptoms and therefore has predictive value.<sup>1, 2</sup> Interestingly, RNA for SARS-CoV-2 was  
21 detected in the submandibular glands and tumor of a patient undergoing tongue surgery for squamous  
22 carcinoma two days before the patient developed symptoms and had a positive nasal swab for the virus:<sup>3</sup>  
23 however, taste tissue was not examined. The sensory symptoms need not be unitary as the virus can  
24 independently target all or any combination of the senses<sup>4,5</sup> and may even cause deficits or changes in a specific  
25 taste quality. Branches of five cranial nerves (CN I [smell], V [chemesthesis: heat, pungency], and VII, IX and  
26 X [taste, Figure 1A] are involved in relaying those specific senses to the central nervous system. Taste is first  
27 discriminated in taste receptor cells (TRCs) within taste buds, which are autonomous organs mostly located in  
28 circumvallate (CV), foliate (FL), and fungiform (F) papillae (P) in the tongue. Each taste bud is supplied by  
29 nerve fibers, a capillary artery and vein. Solitary taste buds are also buried in the epithelial layer of the uvula,  
30 epiglottis, larynx, upper airways and proximal esophagus. TRCs contain the machinery for discriminating five  
31 prototypic tastes that can be appreciated from commonly consumed foods: salty (pretzels), sweet (chocolate,  
32 sugar, artificial sweeteners), bitter (coffee), umami (monosodium glutamate, sweet amino acids) and sour  
33 (citrus); one, more than one or all may be altered (dysgeusia) or absent (ageusia) due to SARS-CoV-2 infection.  
34 Taste buds contain just three distinct types of TRCs for mediating taste discrimination: Type I (salty), Type II  
35 (sweet, bitter and umami; these are discriminated on the basis of specific receptor engagement on the cell  
36 surface while sharing downstream signal transduction mechanisms) and Type III (sour) (Figure 1A).<sup>6, 7</sup> Solitary  
37 chemosensory cells containing similar bitter receptors and signal transduction machinery as are present in Type  
38 II cells reside in trachea, extrapulmonary bronchi and in the lung hilus, where based on rodent investigations  
39 they ‘sense’ the microenvironment and regulate respiration rate through CN X; bitter stimuli and cholinergic  
40 activation lead to decreased respiratory rates.<sup>8</sup> All taste buds have the same three TRC types, though ratios of

cell types vary (Figure 1A). For example, Type I cells are rare in FP.<sup>9</sup> These TRCs are not neurons: they are modified epithelial cells. ACE2 expression has not been found in the neurons of the geniculate ganglion<sup>10, 11</sup> whose fibers innervate the FP *via* CN VII, or in sensory afferents of CN X<sup>12</sup> that innervate the solitary buds of the epiglottis, larynx, and chemosensory cells of the airways. Additionally, CN V neurons, which mediate chemesthesis, do not express ACE2.<sup>13, 14</sup> It therefore seemed unlikely that alterations in taste and chemesthesis are due to SARS-CoV-2 invasion of sensory afferents of four CNs, but more likely due to direct infection of the taste buds, lingual epithelium and oral mucosa. Epithelial cells shed into saliva, the source of which could be lingual epithelium, salivary glands and oral mucosal surfaces, from SARS-CoV-2 infected patients were recently reported to contain low ACE2 expression, and in some cases, viral RNA.<sup>15</sup> TRCs or chemosensory cells were not studied in that report.

## Materials and Methods

### Study design, study population and setting

Human circumvallate papillae (CVP) tissue was obtained from cadaveric tongues and placed in formalin (National Disease Research Interchange) until processing at the NIA. Fresh human fungiform papillae (FP), ≤ eight per participant, were obtained with IRB approval (IRB/NIH # 2018-AG-N010, - N322) and with participants' written consent. All biopsies were carried out in the IRP NIA Clinical Research Unit, Baltimore, MD. FP were excised after topical application of 1% lidocaine using sterile curved spring micro-scissors (McPherson-Vannas, WPI, Sarasota, FL) Type # SR5603 (Roboz Surgical Instrument Co, Gaithersburg, MD). Individual papillae to be used for immunohistochemistry or ISH were immediately placed in 4% paraformaldehyde (PFA, Fisher Scientific, Atlanta, GA), cryoprotected with 20% sucrose (Millipore Sigma, St. Louis, MO) overnight at 4°C and frozen in optimal cutting temperature media (Tissue Tek O.C.T. Compound, Sakura Fintek, St. Torrance, CA) and stored at -80°C until use.

## Immunostaining of human lingual tissue

CVP tissue and FP were cryosectioned (10  $\mu$ m thick) using a Leica CM 1950 cryostat, mounted onto ColorFrost Plus Micro slides (Fisher Scientific) and then stored at -80°C. Immunostaining was performed as described previously.<sup>9</sup> To permeabilize the cells in the tissue, slides were placed in Tris-buffered saline (TBS) (pH, 7.4; Quality Biologicals, Gaithersburg, MD) with 0.2% Triton-X 100 (Millipore Sigma) for 5 minutes at room temperature. They were then washed three times (2 minutes) in TBS. Antigen retrieval was performed by placing the slides in 10 mM of sodium citrate buffer (pH, 6.0; Vector Laboratories, Burlingame, CA) at 95°C for 30 minutes. The slides were left to cool at room temperature in the citrate buffer for a further 30 minutes and were then rinsed in water and then TBS as before. Sections were incubated with normal goat serum block consisting of 2% goat serum, 1% OmniPur® BSA Fraction V (Millipore Sigma), 0.1% gelatin, (Millipore Sigma), 0.1% Triton X-100 (Millipore Sigma), 0.05% Tween 20 (Millipore Sigma), and 0.05% sodium azide (Millipore Sigma) in TBS for 1 hour at room temperature. Sections were then incubated with primary antibodies (Table 1) diluted in the same normal goat serum block at 4°C overnight. Tissue sections were rinsed with TBS with 5% tween (TBST) and incubated for 1 hour with fluorescently labelled secondary antibodies (Table 1) at 1:1000 dilution, then washed with TBST. After nuclear staining (4',6-diamidino-2-phenylindole dihydrochloride, DAPI, Sigma Aldrich) sections were mounted with Fluoromount G (Southern Biotechnology, Birmingham, AL). Controls used were incubation without primary antibody, isotype controls, and pre-absorption with a 5-fold excess of the blocking peptide (ACE2). Appropriate no-primary-antibody controls were prepared with each individual batch of slides. Confocal fluorescence images were captured using Zen Black Version 14 software on a Zeiss LSM-880 (Oberlochen, Germany) confocal microscope, brightness and contrast were adjusted globally. All figures were compiled in Adobe Illustrator 2021 (San Jose, CA)

## RNAscope *in situ* hybridization (ISH)

RNAscope probes were all from Advanced Cell Diagnostics (Newark, CA; Table 2). V-nCoV2019-S (Cat# 848561) is an antisense probe specific to the viral genomic positive strand RNA of the spike protein sequence

20 and V-nCoV2019-orf1ab (Cat# 859151) is a sense probe specific to the viral ORF1ab (Open Reading Frame  
21 lab) negative strand RNA produced when the virus is replicating<sup>16</sup>. Taste receptor cell marker probe for Type I  
22 cell was *ENTPD2* (Cat# 507941), for Type II cell was *PCLB2* (custom designed), and Type III cell was *NCAMI*  
23 (Cat# 421468). *ENTPD2* is translated into ectonucleoside triphosphate diphosphohydrolase 2 which is  
24 expressed only on Type I cells,<sup>17</sup> while *NCAMI* is translated to a neural cell adhesion molecule that is a cell  
25 surface marker for Type III cells.<sup>18</sup> FP were sectioned at 10  $\mu$ m using RNase-free conditions on a Leica CM  
26 1950 cryostat, mounted onto ColorFrost Plus Micro (Fisher Scientific) slides and stored at -80°C in a slide box  
27 that was placed in a sealed Zip-loc™ bag until use. Retrieving mRNA targets from the fixed frozen FP sections,  
28 pretreatment, probe hybridizations, and labeling were all performed according to RNAscope Multiplex  
29 Fluorescent Detection Kit v2 (Cat# 323100) protocol: the negative control probe was a universal control probe  
30 targeting the bacterial *Dapb* gene (GenBank accession number: EF191515) from the *Bacillus subtilis* strain  
31 (Cat# 320871). Positive controls were probes to the human transcripts *POLR2A* (C1) and *PPIB* (C2), and *UBC*  
32 (C3) (Cat# 320861) for RNAscope Multiplex Fluorescent Assay. Images were acquired using Zen software on a  
33 Zeiss LSM 880 confocal microscope.

### 35 **Quantification of Percentages of Proliferating Cells**

36 The numbers of cells positive for Ki67 and phosphorylated histone H3 (PHH3) were determined using the  
37 Cytonuclear FL algorithm in the HALO® image analysis software platform (HALO platform 2.2, Indica Labs,  
38 Albuquerque, NM) that identified Ki67-positive nuclei (green), PHH3-positive nuclei (red), and DAPI stained  
39 nuclei (blue) on immunostained sections imaged on the LSM 880 using the 20X objective. The percentage of  
40 Ki67 positive cells was determined as a percentage of the total number of DAPI positive nuclei. The percentage  
41 of Ki67 positive cells positive for the mitotic marker PHH3 was also determined. Cells in three to four sections  
42 from each of 2 FPs per individual were counted. One-way analysis of variance (ANOVA) with Tukey's  
43 multiple comparison was performed using GraphPad Prism 9 (GraphPad Software Inc., San Diego, CA). The  
44 data are presented as mean  $\pm$ SEM and  $p < 0.05$  is considered statistically significant.

## Results

Humans have approximately 5,000-10,000 taste buds, of which about half are buried on the sides of CVP (Figure 1A, B).<sup>19</sup> The presence of ACE2 in taste buds within CVP of post-mortem tissue was investigated by immunofluorescent staining (IFS) and found it to be co-expressed with phospholipase C  $\beta_2$  (PLC $\beta_2$ ), a marker and obligatory signal transduction molecule in Type II TRCs (Figure 1B, top panel)<sup>20</sup>. Taste buds within FLPs, which are vertical folds on the sides of the tongue, were not sufficiently preserved for definitive ACE2 IFS. Obtaining fresh FP, on the other hand, is a relatively simple biopsy procedure. There are 150-200 FP on the front half of the tongue and each FP contains zero to two buds maximum on its surface (Figure 1B, bottom panel, for example). TRCs are replaced approximately every 14 days from replicating stem cells underneath the epithelial layer of FP.<sup>21</sup> ACE2 was found to be present in TRCs within taste buds of freshly biopsied FP, where again it colocalized with PLC $\beta_2$  by IFS (Figure 1B, bottom panel). This was confirmed by *in situ* hybridization (ISH; Figure 1C, top panel and middle panel), note the presence of ACE2 in the area outside of the taste bud. It therefore seems evident that taste buds provide a portal for SARS-CoV-2 entry. ACE2 (note white arrows) was not found to be co-expressed with Types I and III cell markers (ISH; Figure 1C, bottom two panels).

Participant #114 (female with controlled hypertension, 45yrs old) in the study contracted SARS-CoV-2 (SARS-CoV-2<sup>+</sup> by PCR) and she reported changes in sweet taste (chocolate did not taste like chocolate) and in chemesthesis (a curry meal tasted 'white') beginning 15 days previously. Her tongue had enlarged, red-appearing FP, contrasting with the shiny condition of her FP 3 months later (Figure 2A). Four FP were removed for histology. Of these four FP, just one contained taste buds (Figure 2B). An RNAscope antisense probe specific to the genomic positive strand RNA (for proof of viral infection) of the spike protein (S) sequence of SARS-CoV-2 and a sense probe specific to the *ORF1ab* negative strand RNA (for proof of viral replication) indicated the presence of replicating SARS-CoV-2 in *PLCB2* positive cells (participant #114; Figure 2C). Note the arrow pointing to another viral positive cell in the neighboring taste bud. A sex- and age-matched control FP was negative for the virus (Supplemental Figure 1A). The virus was present in lamina propria of participant #114 both by ISH and IFS (Supplemental Figure 1B, C respectively). The stem cell layer

70 within the FP of #114 had disruptions based on immunostaining for Ki67 (a marker of cell turnover): this had  
71 improved on a subsequent biopsy 6 weeks later by which time her sense of taste had recovered (Figure 2D, left-  
72 hand side images). An age and sex matched control was used as a healthy control for #114. Participant #089  
73 (male with no pre-existing medical conditions, 63yrs old) first donated FP in 2019 (pre-SARS-CoV-2). He was  
74 biopsied 6 weeks after being SARS-CoV-2<sup>+</sup> by PCR but at a time when he still had mild dysgeusia specifically  
75 his sweet (chocolate was almost tasteless) and bitter (coffee tasted like mud) sensations were still impaired by  
76 history. At this time, his other viral symptoms namely chills, muscle aches, joint pain, brain ‘fog’, had abated  
77 and he had returned to work. He was biopsied again at 10 weeks post SARS-CoV-2. No virus was present in  
78 his FP (Supplemental Figure 1D): however, his stem cell layer had disruptions 6 weeks post infection compared  
79 to 2019 (#089 Pre), and the disruptions were less obvious and taste perception was recovering (coffee was now  
80 perceived as tasteless, but not muddy) at 10 weeks (Figure 1D, right hand side images). The total number of  
81 cells positive for Ki67 (as a percentage of 4',6-diamidino-2-phenylindole DAPI-positive nuclei) and the  
82 percentage of Ki67 cells positive for the mitotic marker phosphorylated histone H3 (PHH3) in 3-4 sections from  
83 each of two FP from participants at the three timepoints shown in Figure 2D were counted (Figure 2E). One-  
84 way ANOVA showed that the percentage of Ki67 positive cells in FP of #114 (during) was significantly lower  
85 than control and 6 weeks post-COVID-19 ( $F_{(2,21)}=25.2$ ,  $p<0.0001$ ). The percentage values of Ki67 positive cells  
86 in FP of participant #089 at 6 and 10 weeks post-COVID-19 were significantly lower than those of his pre-  
87 COVID-19 value ( $F_{(2,18)}=6.97$ ,  $p=0.0057$ ). One-way ANOVA also showed the percentage of PHH3/Ki67  
88 positive cells in the FP sections from #114 during the course of COVID-19 was significantly lower than those in  
89 sections taken from the healthy, sex and aged matched control and #114 6 weeks post-COVID-19 ( $F_{(2,21)}=19.35$ ,  
90  $p<0.0001$ ). The percentage of PHH3/Ki67 positive cells in FP sections from #089 at 6 and 10 weeks post-  
91 COVID-19 were significantly lower than those of the pre-COVID-19 FP sample ( $F_{(2,18)}=21.23$ ,  $p<0.0001$ ). A  
92 marker of cellular apoptosis, cleaved caspase 3, was not expressed in the stem cell layer during COVID-19 in  
93 participant #114 or during the period of taste dysfunction of participant #089 as shown in Figure 2F.

## Discussion

We discovered that oral infection and replication with SARS-CoV-2 occurred in taste bud Type II cells. Virus may be transported to the oral cavity on air eddies containing virus in droplets directly into mouth and/or in droplets, nasal mucous or epithelial cells shed from the nose (Figure 1A). While SARS-CoV-2 infection is noted in oral cavity and saliva, no one had shown evidence of its replication in salivary glands, gingiva or oral mucosa, and no one has yet published on taste tissue. Furthermore, previous studies<sup>15, 22, 23</sup> did not address the cellular location of ACE2 within human taste buds using the highly specific techniques of ISH (mRNA) and IFS (protein). Taste buds do not contain a resident immune system<sup>24</sup> and TRCs account for all cells within taste buds. In contrast to SARS-CoV-2 infection in the olfactory system<sup>25</sup> where it is the sustentacular cells that are affected our data show evidence for infection in the taste apparatus *per se i.e.* the taste buds. Replication of virus can likely then occur undisturbed and allow for transmission from the taste bud into circulation, and locally infect lingual and salivary gland epithelium, oral mucosa and larynx and even on into the lungs. TRCs within taste buds contain interferon receptors, and a systemic response to virus should eliminate the virus while simultaneously leading to taste changes.<sup>24</sup> While we did not investigate it directly it is possible that there could be indirect effects on the neuronal<sup>26</sup> or blood supply to the taste buds as is noted by the detection of ACE2 in the proximity of the taste buds. We further propose that deficient stem cell turnover will result in TRCs not being effectively replaced and that this explains why some people have slow recovery of their complete taste repertoire. The detection of actively replicating SARS-CoV-2 in *PLCB2*-containing cells indicates that the virus has a direct route into TRCs via ACE2 on the type II cells. The presence of ACE2 on Type II cells specifically is very intriguing because these are the cells that ‘taste’ amino acids and ACE2 in the gut has been shown to dimerize with amino acid transporters where it plays a vital role in efficient amino acid absorption.<sup>27</sup> We hypothesize that ACE2 is also on the chemosensory cells present in airways as their cellular machinery is similar to Type II cells in taste buds. They contain bitter receptors activated by ligands such cycloheximide, a bitter receptor agonist, and require PLC $\beta_2$  for signal transduction.<sup>8</sup> Therefore, viral infection of those cells might directly decrease respiratory drive, resulting in worsening oxygen desaturation. The role of

20 chemosensory cells in the upper airways or of TRCs in taste buds during SARS-CoV-2 infection has not been  
21 studied because of practical difficulties: obtaining a fresh CVP where numerous taste buds reside and where  
22 they are larger than in FP is not a viable option because CVPs have not been shown to regrow<sup>28</sup>; obtaining FP or  
23 especially fresh tissue from airways in sick people has associated medical conundrums; there is a paucity of  
24 taste buds within FP as there are at most two taste buds but sometimes just one and occasionally none, even in  
25 young people<sup>29</sup>; taste buds may be damaged by virus and not be recognizable, especially to an untrained eye;  
26 taste buds are buried in the epithelial layer where they occupy less than 1% of the total mass of a papilla (Figure  
27 1A, B) and therefore are easily missed if the whole papilla is not systematically sectioned; and finally, even  
28 when present, a taste bud in a FP is approximately 30  $\mu\text{m}$  in diameter, thereby providing a maximum of 3-4  
29 slides with taste bud cells for in depth investigation.

30 In conclusion by demonstrating the co-localization of SARS-CoV-2 virus, Type II taste cell marker and  
31 the viral receptor ACE2, we show evidence for replication of this virus within taste buds that could account for  
32 acute taste changes during active COVID-19. This work also shows that proliferation of the taste stem cells in  
33 recovering patients may take weeks to return to their pre-COVID-19 state, providing a hypothesis for more  
34 chronic disruption of taste sensation, reports of which are now appearing in the medical literature. It is  
35 worthwhile noting that the influenza A virus subtype H3N2 that caused the pandemic of 1968-69 resulted in  
36 long-term alternations of taste and smell in some patients. Patients suffering from post-influenza hypo- and  
37 dysgeusia many years after their infection had disrupted taste bud architecture with decreased numbers of TRCs  
38 and were lacking cilia in the pore region of the taste bud.<sup>30</sup>

## 40 **Acknowledgements**

41 All authors contributed equally. We thank all the participants of the study (2018-AG-N010) and all the IRP NIA  
42 clinical staff.

13

## 14 **References**

15 [1] Menni C, Valdes AM, Freidin MB, Sudre CH, Nguyen LH, Drew DA, Ganesh S, Varsavsky T, Cardoso MJ,  
16 El-Sayed Moustafa JS, Visconti A, Hysi P, Bowyer RCE, Mangino M, Falchi M, Wolf J, Ourselin S, Chan AT,  
17 Steves CJ, Spector TD: Real-time tracking of self-reported symptoms to predict potential COVID-19. *Nature*  
18 *medicine* 2020, 26:1037-40.

19 [2] Melley LE, Bress E, Polan E: Hypogeusia as the initial presenting symptom of COVID-19. *BMJ case*  
20 *reports* 2020, 13.

21 [3] Guerini-Rocco E, Taormina SV, Vacirca D, Ranghiero A, Rappa A, Fumagalli C, Maffini F, Rampinelli C,  
22 Galetta D, Tagliabue M, Ansarin M, Barberis M: SARS-CoV-2 detection in formalin-fixed paraffin-embedded  
23 tissue specimens from surgical resection of tongue squamous cell carcinoma. *J Clin Pathol* 2020, 73:754-7.

24 [4] Adamczyk K, Herman M, Fraczek J, Piec R, Szykula-Piec B, Zaczynski A, Wojtowicz R, Bojanowski K,  
25 Rusyan E, Krol Z, Wierzba W, Franek E: Sensitivity and specificity of prediction models based on gustatory  
26 disorders in diagnosing COVID-19 patients: a case-control study. *medRxiv* 2020:2020.05.31.20118380.

27 [5] Parma V, Ohla K, Veldhuizen MG, Niv MY, Kelly CE, Bakke AJ, Cooper KW, Bouysset C, Pirastu N,  
28 Dibattista M, Kaur R, Liuzza MT, Pepino MY, Schöpf V, Pereda-Loth V, Olsson SB, Gerkin RC, Rohlfes  
29 Domínguez P, Albayay J, Farruggia MC, Bhutani S, Fjaeldstad AW, Kumar R, Menini A, Bensafi M, Sandell  
30 M, Konstantinidis I, Di Pizio A, Genovese F, Öztürk L, Thomas-Danguin T, Frasnelli J, Boesveldt S, Saatci Ö,  
31 Saraiva LR, Lin C, Golebiowski J, Hwang LD, Ozdener MH, Guàrdia MD, Laudamiel C, Ritchie M, Havlíček J,  
32 Pierron D, Roura E, Navarro M, Nolden AA, Lim J, Whitcroft KL, Colquitt LR, Ferdenzi C, Brindha EV,  
33 Altundag A, Macchi A, Nunez-Parra A, Patel ZM, Fiorucci S, Philpott CM, Smith BC, Lundström JN,  
34 Mucignat C, Parker JK, van den Brink M, Schmuker M, Fischmeister FPS, Heinbockel T, Shields VDC, Faraji  
35 F, Santamaría E, Fredborg WEA, Morini G, Olofsson JK, Jalessi M, Karni N, D'Errico A, Alizadeh R,  
36 Pellegrino R, Meyer P, Huart C, Chen B, Soler GM, Alwashahi MK, Welge-Lüssen A, Freiherr J, de Groot JHB,

- 57 Klein H, Okamoto M, Singh PB, Hsieh JW, Reed DR, Hummel T, Munger SD, Hayes JE: More Than Smell-  
58 COVID-19 Is Associated With Severe Impairment of Smell, Taste, and Chemesthesis. *Chemical senses* 2020,  
59 45:609-22.
- 70 [6] Kinnamon SC, Finger TE: Recent advances in taste transduction and signaling. *F1000Research* 2019, 8.
- 71 [7] Roper SD, Chaudhari N: Taste buds: cells, signals and synapses. *Nature reviews Neuroscience* 2017,  
72 18:485-97.
- 73 [8] Krasteva G, Canning BJ, Hartmann P, Veres TZ, Papadakis T, Mühlfeld C, Schliecker K, Tallini YN, Braun  
74 A, Hackstein H, Baal N, Weihe E, Schütz B, Kotlikoff M, Ibanez-Tallon I, Kummer W: Cholinergic  
75 chemosensory cells in the trachea regulate breathing. *Proc Natl Acad Sci U S A* 2011, 108:9478-83.
- 76 [9] Doyle ME, Fiori JL, Gonzalez Mariscal I, Liu QR, Goodstein E, Yang H, Shin YK, Santa-Cruz Calvo S,  
77 Indig FE, Egan JM: Insulin Is Transcribed and Translated in Mammalian Taste Bud Cells. *Endocrinology* 2018,  
78 159:3331-9.
- 79 [10] Dvoryanchikov G, Hernandez D, Roebber JK, Hill DL, Roper SD, Chaudhari N: Transcriptomes and  
80 neurotransmitter profiles of classes of gustatory and somatosensory neurons in the geniculate ganglion. *Nature*  
81 *communications* 2017, 8:760.
- 82 [11] Zhang J, Jin H, Zhang W, Ding C, O'Keefe S, Ye M, Zuker CS: Sour Sensing from the Tongue to the  
83 Brain. *Cell* 2019, 179:392-402.e15.
- 84 [12] Prescott SL, Umans BD, Williams EK, Brust RD, Liberles SD: An Airway Protection Program Revealed  
85 by Sweeping Genetic Control of Vagal Afferents. *Cell* 2020, 181:574-89.e14.
- 86 [13] Nguyen MQ, Le Pichon CE, Ryba N: Stereotyped transcriptomic transformation of somatosensory neurons  
87 in response to injury. *eLife* 2019, 8.
- 88 [14] Nguyen MQ, Wu Y, Bonilla LS, von Buchholtz LJ, Ryba NJP: Diversity amongst trigeminal neurons  
89 revealed by high throughput single cell sequencing. *PloS one* 2017, 12:e0185543.
- 90 [15] Huang N, Pérez P, Kato T, Mikami Y, Okuda K, Gilmore RC, Conde CD, Gasmi B, Stein S, Beach M,  
91 Pelayo E, Maldonado JO, Lafont BA, Jang SI, Nasir N, Padilla RJ, Murrah VA, Maile R, Lovell W, Wallet SM,

32 Bowman NM, Meinig SL, Wolfgang MC, Choudhury SN, Novotny M, Aebermann BD, Scheuermann RH,  
33 Cannon G, Anderson CW, Lee RE, Marchesan JT, Bush M, Freire M, Kimple AJ, Herr DL, Rabin J, Grazioli A,  
34 Das S, French BN, Pranzatelli T, Chiorini JA, Kleiner DE, Pittaluga S, Hewitt SM, Burbelo PD, Chertow D,  
35 Frank K, Lee J, Boucher RC, Teichmann SA, Warner BM, Byrd KM: SARS-CoV-2 infection of the oral cavity  
36 and saliva. *Nature medicine* 2021.

37 [16] Liu J, Babka AM, Kearney BJ, Radoshitzky SR, Kuhn JH, Zeng X: Molecular detection of SARS-CoV-2  
38 in formalin-fixed, paraffin-embedded specimens. *JCI Insight* 2020, 5.

39 [17] Vandenbeuch A, Anderson CB, Parnes J, Enjyoji K, Robson SC, Finger TE, Kinnamon SC: Role of the  
40 ectonucleotidase NTPDase2 in taste bud function. *Proc Natl Acad Sci U S A* 2013, 110:14789-94.

41 [18] Takagi H, Seta Y, Kataoka S, Nakatomi M, Toyono T, Kawamoto T: Mash1-expressing cells could  
42 differentiate to type III cells in adult mouse taste buds. *Anatomical science international* 2018, 93:422-9.

43 [19] Witt M: Anatomy and development of the human taste system. *Handbook of clinical neurology* 2019,  
44 164:147-71.

45 [20] Rössler P, Boekhoff I, Tareilus E, Beck S, Breer H, Freitag J: G protein betagamma complexes in  
46 circumvallate taste cells involved in bitter transduction. *Chemical senses* 2000, 25:413-21.

47 [21] Perea-Martinez I, Nagai T, Chaudhari N: Functional cell types in taste buds have distinct longevities. *PloS*  
48 *one* 2013, 8:e53399.

49 [22] Zhong M, Lin B, Pathak JL, Gao H, Young AJ, Wang X, Liu C, Wu K, Liu M, Chen JM, Huang J, Lee LH,  
50 Qi CL, Ge L, Wang L: ACE2 and Furin Expressions in Oral Epithelial Cells Possibly Facilitate COVID-19  
51 Infection via Respiratory and Fecal-Oral Routes. *Frontiers in medicine* 2020, 7:580796.

52 [23] Sakaguchi W, Kubota N, Shimizu T, Saruta J, Fuchida S, Kawata A, Yamamoto Y, Sugimoto M, Yakeishi  
53 M, Tsukinoki K: Existence of SARS-CoV-2 Entry Molecules in the Oral Cavity. *Int J Mol Sci* 2020, 21.

54 [24] Mazucanti CH, Egan JM: SARS-CoV-2 disease severity and diabetes: why the connection and what is to  
55 be done? *Immunity & ageing : I & A* 2020, 17:21.

- 16 [25] Brann DH, Tsukahara T, Weinreb C, Lipovsek M, Van den Berge K, Gong B, Chance R, Macaulay IC,  
17 Chou HJ, Fletcher RB, Das D, Street K, de Bezieux HR, Choi YG, Risso D, Dudoit S, Purdom E, Mill J,  
18 Hachem RA, Matsunami H, Logan DW, Goldstein BJ, Grubb MS, Ngai J, Datta SR: Non-neuronal expression  
19 of SARS-CoV-2 entry genes in the olfactory system suggests mechanisms underlying COVID-19-associated  
20 anosmia. *Science advances* 2020, 6.
- 21 [26] Ismail, II, Gad KA: Absent Blood Oxygen Level-Dependent Functional Magnetic Resonance Imaging  
22 Activation of the Orbitofrontal Cortex in a Patient With Persistent Cacosmia and Cacogeusia After COVID-19  
23 Infection. *JAMA neurology* 2021.
- 24 [27] Camargo SMR, Vuille-Dit-Bille RN, Meier CF, Verrey F: ACE2 and gut amino acid transport. *Clin Sci*  
25 (Lond) 2020, 134:2823-33.
- 26 [28] Ferrell F, Tsuetaki T: Regeneration of taste buds after surgical excision of human vallate papilla.  
27 *Experimental neurology* 1984, 83:429-35.
- 28 [29] Arvidson K, Cottler-Fox M, Friberg U: Fine structure of taste buds in the human fungiform papilla.  
29 *Scandinavian journal of dental research* 1981, 89:297-306.
- 30 [30] Henkin RI, Larson AL, Powell RD: Hypogeusia, dysgeusia, hyposmia, and dysosmia following influenza-  
31 like infection. *The Annals of otology, rhinology, and laryngology* 1975, 84:672-82.
- 32 [31] Puelles VG, Lütgehetmann M, Lindenmeyer MT, Sperhake JP, Wong MN, Allweiss L, Chilla S,  
33 Heinemann A, Wanner N, Liu S, Braun F, Lu S, Pfefferle S, Schröder AS, Edler C, Gross O, Glatzel M,  
34 Wichmann D, Wiech T, Kluge S, Püeschel K, Aepfelbacher M, Huber TB: Multiorgan and Renal Tropism of  
35 SARS-CoV-2. *The New England journal of medicine* 2020, 383:590-2.
- 36 [32] Yang AC, Kern F, Losada PM, Maat CA, Schmartz G, Fehlmann T, Schaum N, Lee DP, Calcuttawala K,  
37 Vest RT, Gate D, Berdnik D, McNerney MW, Channappa D, Cobos I, Ludwig N, Schulz-Schaeffer WJ, Keller  
38 A, Wyss-Coray T: Broad transcriptional dysregulation of brain and choroid plexus cell types with COVID-19.  
39 *bioRxiv* 2020:2020.10.22.349415.

40 [33] Meinhardt J, Radke J, Dittmayer C, Mothes R, Franz J, Laue M, Schneider J, Brünink S, Hassan O, Stenzel  
41 W, Windgassen M, Röbler L, Goebel H-H, Martin H, Nitsche A, Schulz-Schaeffer WJ, Hakroush S, Winkler  
42 MS, Tampe B, Elezkurtaj S, Horst D, Oesterhelweg L, Tsokos M, Heppner BI, Stadelmann C, Drosten C,  
43 Corman VM, Radbruch H, Heppner FL: Olfactory transmucosal SARS-CoV-2 invasion as port of Central  
44 Nervous System entry in COVID-19 patients. bioRxiv 2020:2020.06.04.135012.

58

59

## 70 **Figure Legends**

71 Figure 1. The receptor for SARS-CoV-2 angiotensin converting enzyme 2 (ACE2) is on Type II taste bud cells  
72 in taste papillae of the tongue.

73 Panel A shows the distribution of taste buds and chemosensory cells in the oropharyngeal cavity and how  
74 inhaled virus may infect the tongue and oropharyngeal areas. Branches of three cranial nerves (CN VII, IX and  
75 X) are involved in relaying taste information to the central nervous system. Taste is first discriminated in taste  
76 receptor cells (TRCs) within taste buds located in circumvallate (CVP), foliate (FLP) and fungiform papillae  
77 (FP) in the tongue. Three defined TRCs relay five prototypic tastes. Stem cells immediately surrounding the

78 taste bud receive signals from taste cells prompting differentiation into a replacement TRC. Circles on tongue,  
79 uvula, epiglottis and oropharyngeal areas represent taste buds and chemosensory cells. Panel B, top row shows

30 hematoxylin and eosin (H&E) and immunofluorescent staining (IFS) of CVP (post-mortem) with taste buds  
31 embedded in the epithelial layer. Keratin 8 (KRT8) is a cytoskeletal marker of all TRCs while phospholipase C

32 beta 2 (PLC $\beta_2$ ) is an obligatory signal molecule in all Type II cells. ACE2 and PLC $\beta_2$  were colocalized (merged  
33 signals) in IFS images. Nuclei are shown in blue stained with 4',6-diamidino-2-phenylindole dihydrochloride

34 (DAPI). Likewise, H&E staining of a fresh FP with two taste buds (insert), and IFS for KRT8, PLC $\beta_2$  and  
35 ACE2 shows co-localization of the latter two proteins. Dashed lines in H&E of CVP and FP indicate the

36 location of the line of stem cells. Panel C shows *in situ* hybridization (ISH) images of FP. Top panel, probes for  
37 *PLCB2* and *ACE2* confirm their co-localization in a fresh FP taste bud, nuclei shown in blue. Note the yellow

38 arrows indicate two areas outside the taste bud where *ACE2* signal is found in the absence of *PLCB2*. Middle  
39 panel, co-localization of *ACE2* and *PLCB2* in the same cell is observed and there is no overlap of the Type III

40 cell marker neural cell adhesion molecule 1 (*NCAM1*, light blue arrows),<sup>7</sup> with either of these two markers.

41 Likewise, bottom panel, shows no overlap of *ACE2* (taste cell positivity indicated by two white arrows) with the  
42 probe for the transcript of the Type I cell marker ectonucleoside triphosphate diphosphohydrolase 2 (*ENTPD2*,

orange arrow)<sup>7</sup> and the Type III marker *NCAM1* (taste cell positivity indicated by two pink arrows). Scale bars = 50 $\mu$ m.

Figure 2. Evidence of SARS-CoV-2 in human FP.

Panel A shows tongue photographs of patient #114 moments prior to biopsy of her FP during the course of COVID-19 and 3 months later. Panel B shows H&E staining of a section through the FP from patient #114 that contained two taste buds; the consecutive section was used for ISH outlining the presence of viral particles (SARS-CoV-2 *S*) probe for the Spike mRNA and the SARS-CoV-2 (*ORF1ab*) probe for the replicating virus, shown in Figure 2C. Panel C, an antisense probe specific to the genomic positive strand RNA of the spike protein (*S*) sequence of SARS-CoV-2 and a sense probe to the SARS-CoV-2 *ORF1ab* negative strand RNA indicate the presence of replicating virus in *PLCB2* positive cells (participant #114). Note the arrow pointing to another viral positive cell in the neighboring taste bud. Panel D demonstrates the proliferation of the stem cell layer of the FP by immunostaining for the marker of all active phases of cell cycle Ki67 and the late G2 and M phase markers phosphorylated histone H3 (PHH3). Top left-sided images show a FP from an age- and sex-matched control participant for #114 compared with during and post SARS-CoV-2 infection. White arrows indicate the breaks in the otherwise continuous layer of stem cells. Right-sided panels show a continuous stem cell layer in participant #089 pre, but multiple breaks especially at 6 weeks, and less at 10 weeks, post SARS-CoV-2. Panel E shows the percentages of total cells (as determined by DAPI stained nuclei) positive for Ki67 and the percentage of Ki67 positive cells that are also positive for PHH3 (mean  $\pm$  SEM, \*\*\*\* =  $p < 0.0001$ , \*\* =  $p < 0.01$ , \* =  $p < 0.05$ ). Panel F shows that the proliferating taste stem cells do not express cleaved Caspase 3. Scale bars = 50 $\mu$ m.

L6

L7

L8

L9

L20

## Tables

Antigen	Source Species	Dilution	Manufacturer; Catalog #; RRID
ACE2	Monoclonal Mouse IgG <sub>2A</sub> Clone # 171606	1:50	R&D Systems (Minneapolis, MN); MAB933; AB_2223153
KRT8	Rat	1:100	DSHB (University of Iowa, IA); TROMA-I; AB_531826
PLC $\beta$ <sub>2</sub>	Rabbit	1:100	Santa Cruz Biotechnology (Dallas, TX); sc- 206; AB_632197
Anti-SARS spike glycoprotein antibody	Mouse	1:100	Abcam (Cambridge, MA); ab272420; N/A <sup>31-3</sup> .
Cleaved- Caspase-3	Rabbit	1:100	Abcam; ab3623; PA5-17869; AB_10984484
Phospho-Histone H3 (Ser10)	Rabbit	1:100	Invitrogen; PA5-17869; AB_10984484
Ki67	Mouse	1:200	Agilent (Santa Clara, CA); M724029-2; AB_2250503
Rabbit IgG	Goat (AlexaFluor 488)	1:1000	Invitrogen; A27034; AB_2536097
Rabbit IgG	Goat (AlexaFluor 568)	1:1000	Invitrogen; A11036; AB_10563566
Mouse IgG2a	Goat (AlexaFluor 568)	1:1000	Invitrogen; A21134; AB_1500825
Rat IgG	Goat (AlexaFluor 647)	1:1000	Invitrogen; A21247; AB_141778
Mouse IgG	Goat (AlexaFluor 488)	1:1000	Invitrogen; A28175; AB_2536161

L21

Table 1 Primary and secondary antibodies used, their dilutions and RRID numbers.

L22

Gene Symbol	ISH probe	Catalog #	Accession number	ZZ probe pairs	Nucleotide position
SARS-CoV-2 ( <i>S</i> )	V-nCoV2019-S <sup>16</sup>	848561-C1	NC_045512.2	20	21,631 - 23,303
SARS-CoV-2 ( <i>ORF1ab</i> )	V-nCoV2019-orf1ab- sense <sup>16</sup>	859151-C2	NC_045512.2	40	1,583 - 4,388

<i>ACE2</i>	Probe-Hs-ACE2	848151-C1	NM_021804.3	20	307 - 1,267
<i>PLCB2</i>	Probe-Hs-PLCB2	Custom-C3	NM_004573.3	13	3,822 - 4,621
<i>ENTPD2</i>	Probe-Hs-ENTPD2	507941-C1	NM_203468.2	20	161 - 1,473
<i>NCAM1</i>	Probe-Hs-NCAM1	421468-C2	NM_001242608.1	20	832 - 1,751

Table 2: RNAscope ISH probes. All probes were used were off the shelf from Advanced Cell Diagnostics with the exception of *PLCB2* which was designed in house by the authors. The website used to obtain the NM accession numbers was <https://www.ncbi.nlm.nih.gov/nucore>

### List of Non-Standard Abbreviations

ACE2	Angiotensin-Converting Enzyme-2
CN	Cranial Nerve
COVID-19	Coronavirus Disease 2019
CV	Circumvallate
CVP	Circumvallate Papilla(e)
ddPCR	Droplet Digital Polymerase Chain Reaction
ENTPD2	Ectonucleoside Triphosphate Diphosphohydrolase 2
FL	Foliate Papilla(e)
FP	Fungiform Papilla(e)
ISH	<i>In-Situ</i> Hybridization
NCAM1	Neural Cell Adhesion Molecule 1
ORF1ab	Open Reading Frame 1ab
PHH3	Phosphohistone H3
PLC $\beta_2$	Phospholipase C $\beta$ 2

41	SARS-CoV-2	Severe Acute Respiratory Syndrome Coronavirus 2
42	TMPRSS	Transmembrane Protease, Serine
43	TRC	Taste Receptor Cell(s)

44

45 Supplemental Figure 1. Panel A shows RNAscope detection in a taste bud of a fungiform papilla (FP) of the  
46 transcript for the type II cell marker *PLCB2* and is the negative non-infected control for the SARS-CoV-2  
47 *ORF1ab* probe in a taste bud biopsied from a non-infected age and sex matched control for #114. Nuclei stained  
48 by DAPI, shown in blue. Panel B shows the sense probe targeting the viral *ORF1ab* mRNA demonstrates  
49 positivity within the lamina propria of participant #114 during infection. Panel C shows immunostaining in red  
50 for the SARS spike protein in the lamina propria of a FP from participant #114 during infection. Panel D there  
51 is no evidence of SARS spike protein in the lamina propria of participant #089 post-COVID-19. Scale bars =  
52 50µm.

53

Figure 1

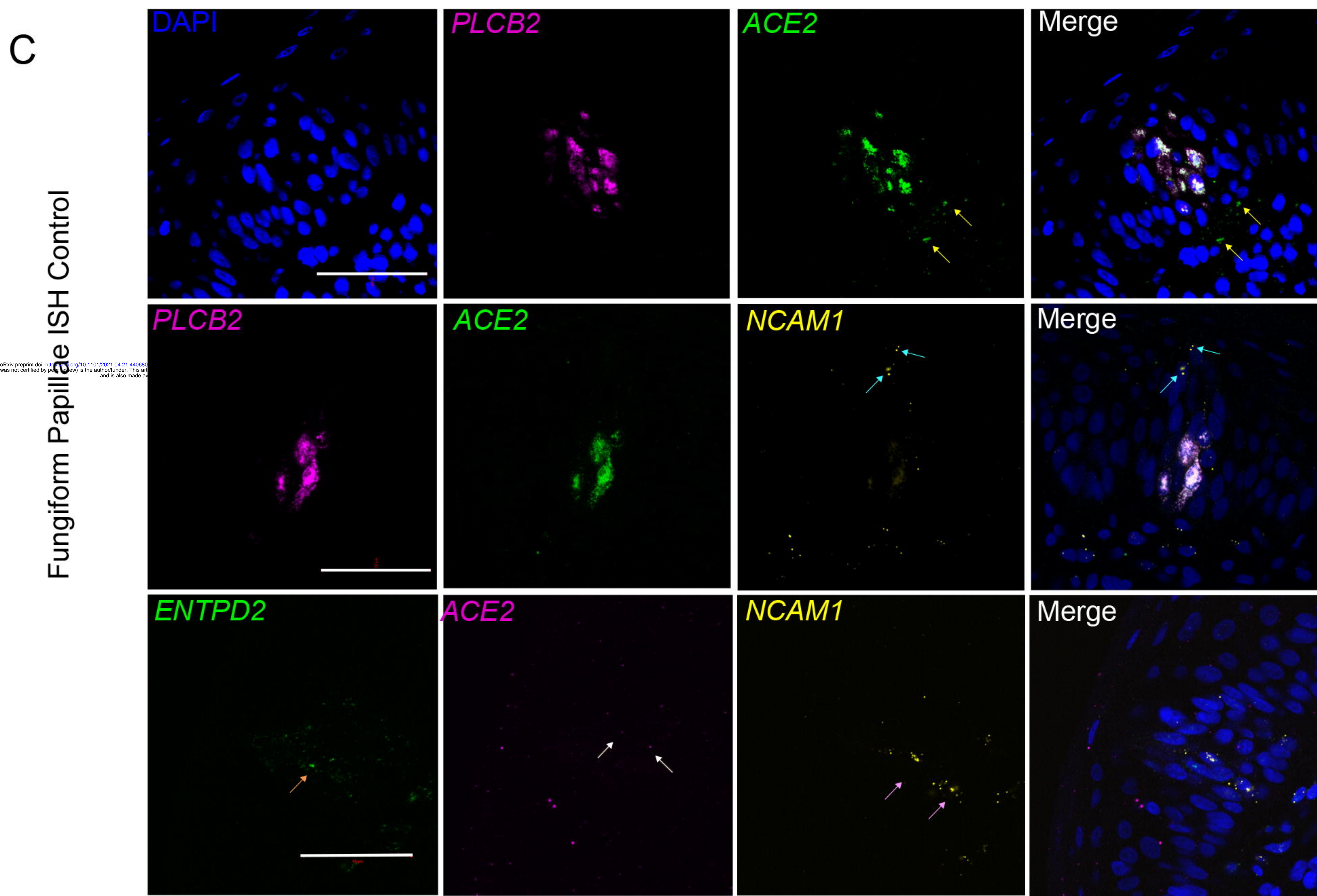
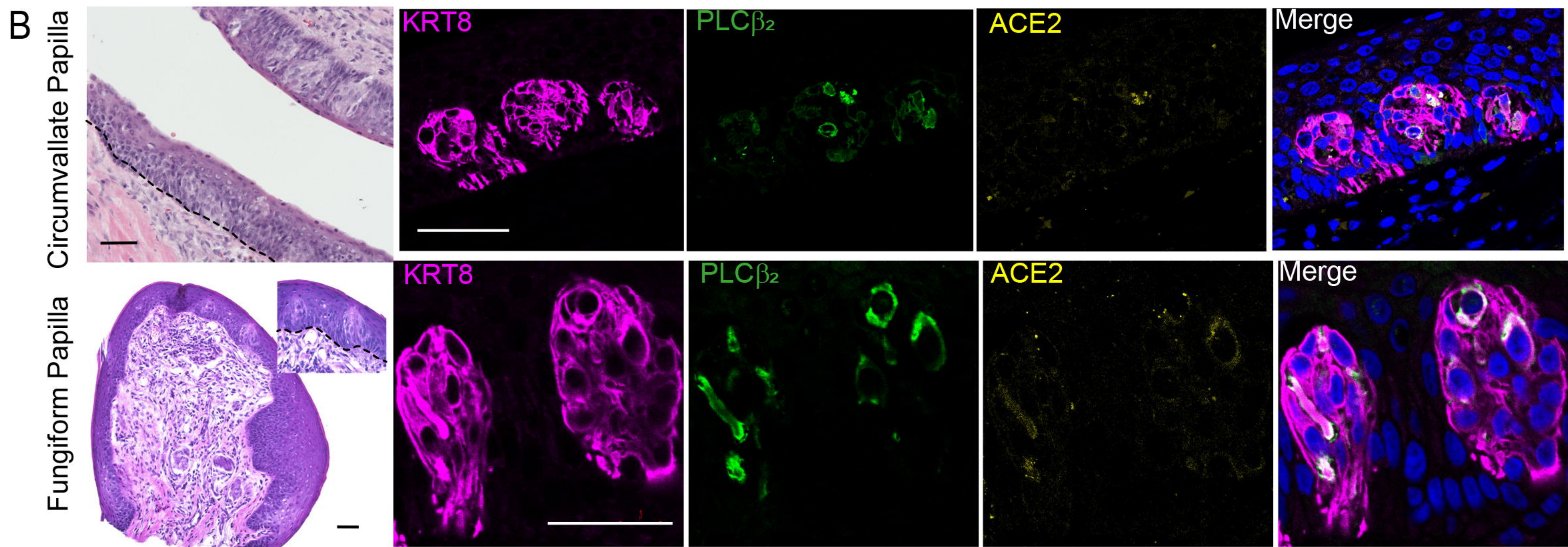
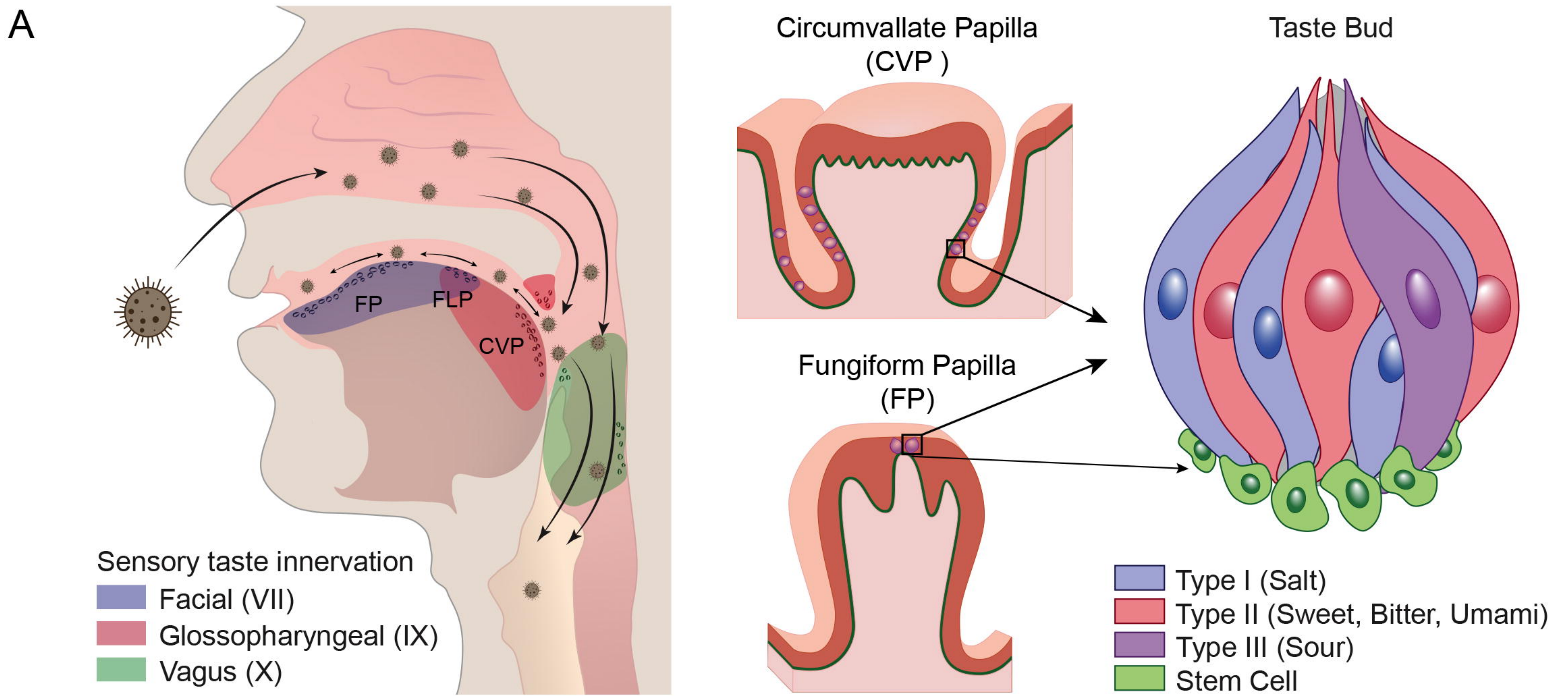


Figure 2

